

## Structure of the Stapled p53 Peptide Bound to Mdm2

Sohee Baek,<sup>†,#</sup> Peter S. Kutchukian,<sup>‡</sup> Gregory L. Verdine,<sup>‡</sup> Robert Huber,<sup>†,§,||,⊥</sup> Tad A. Holak,<sup>†,▽</sup> Ki Won Lee,<sup>#</sup> and Grzegorz M. Popowicz<sup>\*,†</sup>

<sup>†</sup>Max Planck Institute for Biochemistry, Am Klopferspitz 18, 82152 Martinsried, Germany

<sup>‡</sup>Department of Chemistry and Chemical Biology, Harvard University, Cambridge, Massachusetts 02138, United States

<sup>§</sup>Department of Chemistry, Technical University of Munich, Lichtenbergstraße 4, 85748 Garching, Germany

<sup>||</sup>School of Biosciences, Cardiff University, Cardiff CF10 3US, Wales, U.K.

<sup>⊥</sup>Center for Medical Biotechnology, University of Duisburg-Essen, 45117 Essen, Germany

<sup>#</sup>Department of Agricultural Biotechnology, Seoul National University, Seoul 151-921, Republic of Korea

<sup>▽</sup>Faculty of Chemistry, Jagiellonian University, Ingardena 3, 30-060 Cracow, Poland

### S Supporting Information

**ABSTRACT:** Mdm2 is a major negative regulator of the tumor suppressor p53 protein, a protein that plays a crucial role in maintaining genome integrity. Inactivation of p53 is the most prevalent defect in human cancers. Inhibitors of the Mdm2–p53 interaction that restore the functional p53 constitute potential nongenotoxic anticancer agents with a novel mode of action. We present here a 2.0 Å resolution structure of the Mdm2 protein with a bound stapled p53 peptide. Such peptides, which are conformationally and proteolytically stabilized with all-hydrocarbon staples, are an emerging class of biologics that are capable of disrupting protein–protein interactions and thus have broad therapeutic potential. The structure represents the first crystal structure of an *i, i + 7* stapled peptide bound to its target and reveals that rather than acting solely as a passive conformational brace, a staple can intimately interact with the surface of a protein and augment the binding interface.

In tumors where the p53 protein is not mutated (ca. 50% of all cancers), its function is often impaired by increased levels of its negative regulators.<sup>1</sup> One of the principal p53 modulators, the E3 ubiquitin ligase Mdm2, binds directly to the p53 transactivation domain and targets p53 for proteasomal degradation.<sup>2</sup> Reactivation of p53 by inhibiting its binding to Mdm2 is therefore a promising and confirmed approach to cancer therapy.<sup>3</sup> Several small molecules<sup>4,5</sup> and peptidic inhibitors have been developed for this purpose.<sup>6,7</sup> While peptidic inhibitors based on the modified p53 sequence offer very high affinity toward Mdm2, they suffer from low cell permeability and are proteolytically unstable. A successful attempt to overcome these problems has recently been made by designing cyclic peptides that are closed by an all-hydrocarbon “staple”.<sup>8–12</sup> The staple stabilizes the helical structure of the peptide,<sup>8,13</sup> a feature which likely contributes to the enhanced affinity of the peptide for Mdm2 relative to the wild-type peptide.<sup>10</sup> Importantly, the most effective stapled-peptide Mdm2 inhibitor, SAH-p53-8, also targets MdmX and demonstrates cytotoxicity toward cancer cells overexpressing

Mdm2, MdmX, or both.<sup>14</sup> Here we report the X-ray structure of SAH-p53-8 in complex with the human Mdm2 protein.

The bound SAH-p53-8 forms a compact, short, two-turn  $\alpha$ -helix (Figure 1). The peptide is cyclized by an all-hydrocarbon staple introduced before Asn20 (residue numbering as in the native p53 sequence is used) and after Leu26 (Figure 2A). Circular dichroism studies demonstrated that the staple stabilizes the helical state of the unbound peptide.<sup>10</sup> Crystallographic studies of high-affinity p53 analogue peptides revealed extended helicity in the bound state relative to the wild-type peptide.<sup>15</sup> Furthermore, molecular dynamics (MD) simulations of the stapled p53 peptides anticipated elongation of the helical fold relative to the wild-type peptide.<sup>16</sup> Our present structure confirms this prediction and reveals that SAH-p53-8 is the only peptide with a known crystallographic structure that extends its helicity from residue 19 to 27 in the bound state (Figure 2A). None of the other peptides, including those with higher reported affinities toward Mdm2, forms the helix beyond position 24. In the native p53 peptide, Leu26 has  $\Phi/\Psi$  angles in the  $\beta$ -strand region ( $-94^\circ/148^\circ$ , respectively).<sup>17</sup> Stapling of the peptide imposes perfectly helical angles ( $-58^\circ/-45^\circ$ ) on Leu26 in the structure of SAH-p53-8. The structures of other peptides fall somewhere between these two extremes (Figure 2).<sup>15,18,19</sup> The residues outside the stapled part of the sequence are not visible in the electron density map, indicating that they are conformationally flexible in the bound state. This feature is shared by non-cross-linked peptides, where residues outside Phe19–Leu26 range are either flexible or acquire conformations determined by crystal packing. Mdm2 retains its native fold observed in other structures and undergoes only minor ligand-induced changes upon binding SAH-p53-8. Namely, the Met62 side chain folds away from the p53 binding pocket to make room for the aliphatic staple, Val93 shifts toward the inside of the binding pocket by 1.0 Å, and the Tyr100 side chain is in the so-called “closed” conformation.<sup>20</sup> These features are observed in most of the Mdm2 structures.<sup>15,18,19</sup>

The stapled peptide helix is located over the p53 binding pocket and positions in the “correct” orientation the three p53

Received: October 4, 2011

Published: December 8, 2011

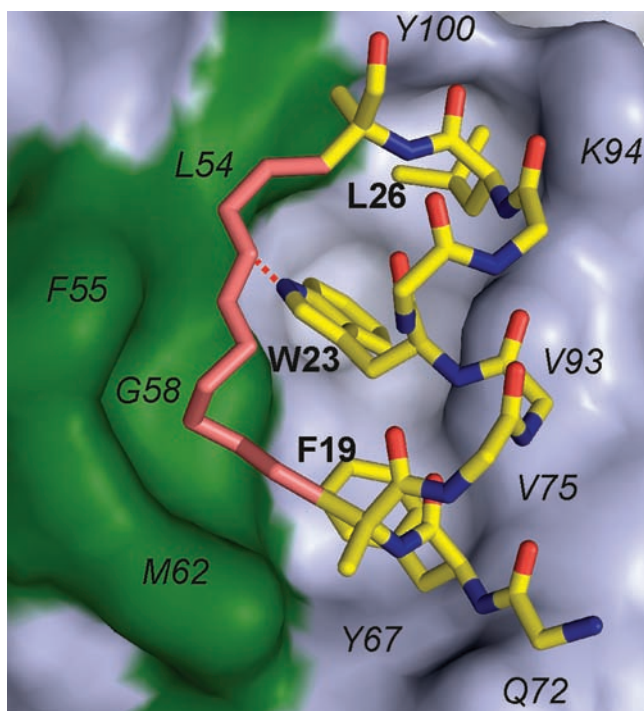


**Figure 1.** Structure of the complex between Mdm2 and the stapled peptide SAH-p53-8. The Mdm2 molecule is shown in the surface representation. Residues of Mdm2 forming the rim of the binding pocket are labeled in italics. SAH-p53-8 uses its Phe19, Trp23, and Leu26 to fill the binding site in a manner similar to the native p53 peptide. The Trp23 indole ring is bound to Leu54 by a hydrogen bond (red dashed line). The aliphatic staple (salmon) protects this hydrogen bond and forms extended hydrophobic contacts with Leu54, Phe55, Gly58, and Met62 of Mdm2 (green surface).

residues that are critical for the binding (Phe19, Trp23, and Leu26). In comparison with the native p53 structure,<sup>17</sup> the whole helix is moved by ca. 1 Å along its long axis toward its N-terminus of p53 (Figure 2B). It is also rotated by 18° counterclockwise around the long axis when looking from the N-terminus toward the C-terminus. This is a unique feature of the stapled peptide, as most of the high-affinity p53 analogue peptides retain an orientation virtually identical to that of the native peptide. Phe19 is located in its Mdm2 pocket in a similar position as the p53 phenylalanine. The plane of its aromatic ring is shifted by 0.6 Å, following the shift of the helix. The Trp23 indole ring plane is identical to the native one but is again rotated to follow the different helix orientation. The hydrogen bond between the indole nitrogen of Trp 23 and the carbonyl oxygen of Leu54 in Mdm2 is preserved in this structure and is 2.82 Å in length. Interestingly, Leu26 fills its pocket in a way that is completely different from the native one. The native p53 lacks helical structure at this residue, while the stapled peptide maintains it (Figure 2A). The position of the Leu26 C $\alpha$  in SAH-p53-8 is therefore moved by 2.7 Å toward the N-terminus of the peptide. Therefore, the side chain of Leu26 is flipped by nearly 180° to fill the same pocket space. No other known structure shares this feature.

The aliphatic staple intimately interacts with the protein, as predicted by MD simulations.<sup>16</sup> It is located directly over the Met50–Lys64 helix that forms the rim of the p53 binding pocket. The staple contributes ca. 10% of the total surface contact area between the peptide and Mdm2. It protects the hydrogen bond between Trp23 and Leu54 from solvent

PDB ID	Sequence	Affinity [nM]	Ref.
	Sec. structure		
	19 23 26		
1YCR	SQETFSDLWKLLPEN --HHHHHTTS--	700	17
3G03	LTFEHYWAQLTS --HHHHHTT--	3.6	15
3EQS	TSFAEYWNLLSP --HHHHHTT--	3.3	19
3JZS	ETFEHWWSQLLS --HHHHHTT--	19.6	18
	└──────────┘		
SAH-p53-8	QSQQTF*NLWRL*QN -HHHHHHHHH	55	10

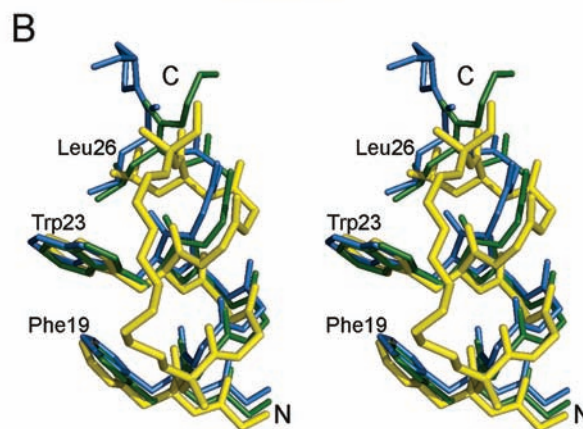


**Figure 2.** Architecture of different p53 peptide analogues. (A) Sequence alignment of the native p53 peptide (PDB entry 1YCR), high-affinity peptides using natural amino acids (PDB entries 3JZS and 3EQS), and the stapled peptide SAH-p53-8. The p53 residues Phe19, Trp23, and Leu26 (highlighted in gray) are critical for binding to Mdm2. The structured residues are presented in bold. A high helical content correlates with increased affinity toward Mdm2. Only the stapled peptide maintains the helical pattern up to Leu26 and beyond. (B) Comparison of the structures of the native p53 peptide (blue), a high-affinity peptide (PDB entry 3G02, green), and the stapled peptide (yellow). The aliphatic staple encompasses two helical turns, effectively “compressing” and strengthening the helix. Leu26 has to assume a different conformation to fill its pocket correctly. The other peptides gradually lose their helical pattern after Trp23. The staple stabilizes the peptide structure, thereby reducing the entropic cost of binding and thus improving the affinity.

competition, likely improving its binding contribution. A unique feature of the structure is an extended hydrophobic interface of the staple linker with Leu54, Phe55, Gly58, and Met62 of Mdm2 (Figure 1). Furthermore, in most known Mdm2 structures, a water molecule is hydrogen-bonded to the Gln59 N and Phe55 O atoms, competing with their direct,  $\alpha$ -helix-forming bond. The staple displaces this water molecule, which likely entropically stabilizes the complex,<sup>21</sup> and also shields the direct Gln59 N–Phe55 O bond. Taken together, these results indicate that the staple–Mdm2 interaction undoubtedly contributes to the tight binding of the SAH-p53-8 peptide.

In addition to SAH-p53-8, several stapled peptides were experimentally investigated (Table 1),<sup>10</sup> and molecular modeling studies suggested that the placement of the staple was one of the dominating factors in the structure–affinity

**Table 1. Staple Attachment, Helicity, and Mdm2 Affinity of SAH Peptides<sup>10</sup>**

peptide	sequence <sup>a</sup>	$\alpha$ helicity	$K_d$ (nM)
WT p53	LSQETFSDLWKLLEN	11%	410
SAH-p53-1	LSQETFSD*WKLLE*	25%	100
SAH-p53-2	LSQE*FSDLWK*LPEN	10%	400
SAH-p53-3	LSQ*TFSDLWKL*EN	12%	1200
SAH-p53-4	LSQETF*DLWKL*EN	59%	0.92
SAH-p53-5	LSQETF*NLWKL*QN	20%	0.8
SAH-p53-6	LSQQT*NLWRL*QN	14%	56
SAH-p53-7	QSQQT*NLWKL*QN	36%	50
SAH-p53-8	QSQQT*NLWRL*QN	85%	55

<sup>a</sup>Staple attachment positions are indicated by \*.

relationships (SARs) displayed by these peptides.<sup>16</sup> Indeed, modeled peptides with staples that “drape” over the protein (e.g., SAH-p53-4–8) experimentally bind Mdm2 with high affinity, while modeled peptides with staples that point out into the solvent (e.g., SAH-p53-1–3) experimentally bind with low affinity. Our structure affirms this interaction for SAH-p53-8 and suggests that if staples are incorporated into future peptide designs, such as reverse<sup>22</sup> or retro-inverso peptides<sup>23,24</sup> aimed at targeting Mdm2, such peptides might profit from placing the staple in such a way that it preserves this beneficial interaction.

One goal of stapling the p53 peptide was to increase its helical content in the unbound state, thereby enhancing its affinity for Mdm2.<sup>10</sup> Our study reveals two accompanying outcomes of stapling. First, the staple makes hydrophobic contacts with the rim of the Mdm2 binding site, likely enhancing the binding affinity. This may also contribute to the 18° rotation observed for the stapled peptide relative to the wild-type peptide. This type of intimate staple-protein hydrophobic–hydrophobic interaction was also observed in the crystal structure of the stapled MCL-1 BH3 helix (MCL-1 SAHB<sub>D</sub>) in complex with MCL-1.<sup>25</sup> In addition, hydrophobic interactions between the staple of the stapled NR box peptides (SP1 and SP2) and the estrogen receptor have been observed, and in the case of SP1, these interactions resulted in a ca. 90° rotation of the helix and a shift in register of 1 position of residues relative to the wild-type peptide.<sup>26</sup> Second, the staple constrains the peptide to a more helical state in the bound conformation in comparison with non-cross-linked peptides, resulting in a conformational change in Leu26, a residue that plays a critical role in binding Mdm2. This suggests that future stapled p53 peptide designs might benefit from incorporating a less restrictive staple. A longer *i, i + 7* staple, perhaps 1–2 methylene units longer, might still enhance the peptide’s affinity for Mdm2 through preorganization of the folded state while allowing Leu26 to bind in its native rotameric state. Indeed, previous experimental studies suggest that longer *i, i + 7* staples increase the helical content relative to the wild-type peptide.<sup>8</sup> Our study supports the notion that in addition to enhancing a peptide’s affinity for a protein by preorganizing the unbound state as an  $\alpha$ -helix, a staple can confer enhanced affinity for a target through hydrophobic contacts with a protein and can perturb the structure of the bound peptide relative to the wild-type structure.

## ■ ASSOCIATED CONTENT

### Ⓢ Supporting Information

Protein production, peptide synthesis, and crystallographic analysis. This material is available free of charge via the Internet

at <http://pubs.acs.org>. The structure has been deposited in the Protein Data Bank as PDB entry 3V3B.

## ■ AUTHOR INFORMATION

### Corresponding Author

popowicz@biochem.mpg.de

## ■ ACKNOWLEDGMENTS

This work was supported by the Deutsche Krebshilfe (Grant 108354) and by the High-Tech Industry Multidisciplinary Research Fund from Dana-Farber Cancer Institute.

## ■ REFERENCES

- (1) Vousden, K. H.; Lane, D. P. *Nat. Rev. Mol. Cell Biol.* **2007**, *8*, 275–283.
- (2) Wade, M.; Wang, Y. V.; Wahl, G. M. *Trends Cell Biol.* **2010**, *20*, 299–309.
- (3) Brown, C. J.; Lain, S.; Verma, C. S.; Fersht, A. R.; Lane, D. P. *Nat. Rev. Cancer* **2009**, *9*, 862–873.
- (4) Vassilev, L. T. *Trends Mol. Med.* **2007**, *13*, 23–31.
- (5) Shangary, S.; Wang, S. *Annu. Rev. Pharmacol. Toxicol.* **2009**, *49*, 223–241.
- (6) Brown, C. J.; Cheok, C. F.; Verma, C. S.; Lane, D. P. *Trends Pharmacol. Sci.* **2011**, *32*, 53–62.
- (7) Popowicz, G. M.; Dömling, A.; Holak, T. A. *Angew. Chem., Int. Ed.* **2011**, *50*, 2680–2688.
- (8) Schafmeister, C. E.; Po, J.; Verdine, G. L. *J. Am. Chem. Soc.* **2000**, *122*, 5891–5892.
- (9) Walensky, L. D.; Kung, A. L.; Escher, I.; Malia, T. J.; Barbuto, S.; Wright, R. D.; Wagner, G.; Verdine, G. L.; Korsmeyer, S. J. *Science* **2004**, *305*, 1466–1470.
- (10) Bernal, F.; Tyler, A. F.; Korsmeyer, S. J.; Walensky, L. D.; Verdine, G. L. *J. Am. Chem. Soc.* **2007**, *129*, 2456–2457.
- (11) Verdine, G. L.; Walensky, L. D. *Clin. Cancer Res.* **2007**, *13*, 7264–7270.
- (12) Verdine, G. L.; Hilinski, G. J. *Methods Enzymol.* **2012**, in press.
- (13) Kutchukian, P. S.; Yang, J. S.; Verdine, G. L.; Shakhnovich, E. I. *J. Am. Chem. Soc.* **2009**, *131*, 4622–4627.
- (14) Bernal, F.; Wade, M.; Godes, M.; Davis, T. N.; Whitehead, D. G.; Kung, A. L.; Wahl, G. M.; Walensky, L. D. *Cancer Cell* **2010**, *18*, 411–422.
- (15) Czarna, A.; Popowicz, G. M.; Pecak, A.; Wolf, S.; Dubin, G.; Holak, T. A. *Cell Cycle* **2009**, *8*, 1176–1184.
- (16) Joseph, T. L.; Lane, D.; Verma, C. S. *Cell Cycle* **2010**, *9*, 4560–4568.
- (17) Kussie, P. H.; Gorina, S.; Marechal, V.; Elenbaas, B.; Moreau, J.; Levine, A. J.; Pavletich, N. P. *Science* **1996**, *274*, 948–953.
- (18) Phan, J.; Li, Z.; Kasprzak, A.; Li, B.; Sebt, S.; Guida, W.; Schönbrunn, E.; Chen, J. *J. Biol. Chem.* **2010**, *285*, 2174–2183.
- (19) Pazgier, M.; Liu, M.; Zou, G.; Yuan, W.; Li, C.; Li, C.; Li, J.; Monbo, J.; Zella, D.; Tarasov, S. G.; Lu, W. *Proc. Natl. Acad. Sci. U.S.A.* **2009**, *106*, 4665–4670.
- (20) Popowicz, G. M.; Czarna, A.; Rothweiler, U.; Szwagierczak, A.; Krajewski, M.; Weber, L.; Holak, T. A. *Cell Cycle* **2007**, *6*, 2386–2392.
- (21) (a) Connelly, P. R.; Aldape, R. A.; Bruzzese, F. J.; Chambers, S. P.; Fitzgibbon, M. J.; Fleming, M. A.; Itoh, S.; Livingston, D. J.; Navia, M. A.; Thomson, J. A.; Wilson, K. P. *Proc. Natl. Acad. Sci. U.S.A.* **1994**, *91*, 1964–1968. (b) Dunitz, J. D. *Science* **1994**, *264*, 670–670.
- (22) Placzek, W. J.; Sturlese, M.; Wu, B.; Cellitti, J. F.; Wei, J.; Pellecchia, M. *J. Biol. Chem.* **2011**, *286*, 39829–39835.
- (23) Sakurai, K.; Chung, H. S.; Kahne, D. J. *J. Am. Chem. Soc.* **2004**, *126*, 16288–16289.
- (24) Li, C.; Pazgier, M.; Li, J.; Li, C.; Liu, M.; Zou, G.; Li, Z.; Chen, J.; Tarasov, S. G.; Lu, W.-Y.; Lu, W. *J. Biol. Chem.* **2010**, *285*, 19572–19581.
- (25) Stewart, M. L.; Fire, E.; Keating, A. E.; Walensky, L. D. *Nat. Chem. Biol.* **2010**, *6*, 595–601.

(26) Phillips, C.; Roberts, L. R.; Schade, M.; Bazin, R.; Bent, A.; Davies, N. L.; Moore, R.; Pannifer, A. D.; Pickford, A. R.; Prior, S. H.; Read, C. M.; Scott, A.; Brown, D. G.; Xu, B.; Irving, S. L. *J. Am. Chem. Soc.* **2011**, *133*, 9696–9699.